Glutathione Content as a Potential Mediator of the Vulnerability of Cultured Fetal Cortical Neurons to Ethanol-Induced Apoptosis

Shivani Kaushal Maffi[1,*], **Mary Latha Rathinam**[2], **Priscilla P. Cherian**[2], **William Pate**[1], **Rhoda Hamby-Mason**[2], **Steven Schenker**[2], and **George I. Henderson**[2]

[1]Department of Medicine, Division of Infectious Diseases, University of Texas Health Science Center, San Antonio, Texas

[2]Department of Medicine, Division of Gastroenterology and Nutrition, University of Texas Health Science Center, San Antonio, Texas

Abstract

Ethanol ingestion during pregnancy elicits damage to the developing brain, some of which appears to result from enhanced apoptotic death of neurons. A consistent characteristic of this phenomenon is a highly differing sensitivity to ethanol within specific neuron populations. One possible explanation for this "selective vulnerability" could be cellular variations in glutathione (GSH) homeostasis. Prior studies have illustrated that ethanol elicits apoptotic death of neurons in the developing brain, that oxidative stress may be an underlying mechanism, and that GSH can be neuroprotective. In the present study, both multiphoton microscopy and flow cytometry demonstrate a striking heterogeneity in GSH content within cortical neuron populations. Ethanol differentially elicits apoptotic death and oxidative stress in these neurons. When neuron GSH content is reduced by treatment with butathione sulfoxamine, the ethanol-mediated enhancement of reactive oxygen species is exacerbated. Sorting of cells into high- and low-GSH populations further exemplifies ethanol-mediated oxidative stress whereby apoptotic indices are preferentially elevated in the low-GSH population. Western blot analysis of the low-GSH subpopulations shows higher ethanol-mediated expression of active caspase 3 and 24-kDa PARP-1 fragments compared with the high-GSH subpopulation. In addition, neuronal content of 4-hydroxynonenal adducts is higher in low-GSH neurons in response to ethanol. These studies suggest that GSH content is an important predictor of neuronal sensitivity to ethanol-mediated oxidative stress and subsequent cell death. The data support the proposition that the differences in proapoptotic responses to ethanol within specific neuron populations reflect a heterogeneity of neuron GSH content.

Keywords

FASD; apoptosis; oxidative stress; glutathione; alcohol; neuron

The toxic effects of maternal alcohol consumption on the fetus are well documented both in animal and in human models. Depending on the severity of these responses, the outcomes are collectively termed *fetal alcohol syndrome* (FAS), *fetal alcohol effects*, or the more recently coined term *fetal alcohol spectrum disorders* (FASD; Streissguth, 1997; Mattson and Riley, 1998; Sokol et al., 2003). Central among the responses to in utero alcohol exposure are neurodevelopmental deficits affecting multiple regions of the central nervous

*Correspondence to: Shivani Kaushal Maffi, PhD, Department of Medicine, Division of Infectious Diseases, University of Texas Health Science Center at San Antonio, 7703 Floyd Curl Drive, San Antonio, TX 78229. maffi@uthscsa.edu.
The first two authors contributed equally to this work.

system (CNS), including the cerebellum, hippocampus, olfactory bulbs, and cerebral cortex (Barnes and Walker, 1981; West et al., 1990; Goodlett et al., 1991; Miller and Kuhn, 1995; Bearer et al., 1999; Chen et al., 2003). In vivo and in vitro studies suggest that developmental deficits in these regions can be linked to reduced progenitor cell proliferation, neuron translocation, and enhanced neuron death (Gressens et al., 1992; Miller, 1996; Moore et al., 1999; Olney et al., 2001; Jacobs and Miller, 2001; He et al., 2005). Although both glia and neurons are affected by ethanol, the latter are typically addressed as primary targets (Miller and Potempa, 1990; Luo et al., 1997; Chandler et al., 1997; Crews et al., 1999; Jacobs and Miller, 2001).

During normal fetal brain development, about 50% of CNS neurons are culled by apoptotic death (Sastry and Rao, 2000). Ethanol enhances the number of neurons undergoing programmed cell death, and this increase in neuron loss is critically dependent on the dose and duration of ethanol exposure (Maier and West, 2001; Olney et al., 2002; Young and Olney, 2006). In vivo, very high levels of ethanol can elicit massive losses of neurons via apoptotic death (Young et al., 2003); however, more moderate and clinically relevant concentrations can also generate an enhanced apoptotic loss of neurons, albeit to a more modest degree (Mooney and Miller, 2001; Young et al., 2005). In the latter setting, it was clear that ethanol induced apoptotic death in small fractions of neurons in specific populations. This has also been illustrated in highly pure cultures of neurons and in brain slices, in which there appear to be subpopulations of neurons that readily respond to ethanol-mediated apoptotic death (Ikonomidou et al., 2000; Ramachandran et al., 2003; Young and Olney, 2006). Mechanisms underlying this varying apoptotic sensitivity of neurons to ethanol have not been established. Ethanol can elicit oxidative stress in cultured fetal rat cortical neurons, and the response varies from rapid (minutes of exposure) and striking to no response at all (Ramachandran et al., 2003). The induction of oxidative stress is an initial event followed by activation of apoptotic machinery and eventual cell death. Importantly, the cascade of apoptotic events can be prevented by normalization of neuronal GSH content, either by pretreatment with N-acetylcysteine (Ramachandran et al., 2003) or by coculturing with astrocytes (Watts et al., 2005; Rathinam et al., 2006). This both supports a causal role for oxidative stress in ethanol-induced apoptotic neuron death and suggests that neuron sensitivity to ethanol could be mediated by cellular GSH content. The following studies demonstrate that this selective vulnerability of neurons to ethanol-mediated apoptotic death may reflect a wide variability in baseline neuron GSH content in which the neurons with the lowest GSH are those that succumb to ethanol most readily.

MATERIALS AND METHODS

Materials

Minimum essential medium (MEM), fetal bovine serum (FBS), monochlorobimane (MCB), 2′,7′-dichlorodihydro-fluorescein diacetate (DCF-DA), and secondary Alexa conjugates were purchased from Invitrogen (Carlsbad, CA), and Vectashield was obtained from Vector Laboratories (Burlin-game, CA). Horse serum (HS), bovine serum albumin (BSA), and poly-D-lysine were from Sigma (St. Louis, MO). The kit for protein estimation was from Bio-Rad (Hercules, CA). The antibody against HNE was a generous gift from the late Dr. Herman Esterbauer. Caspase-3 was from Cell Signaling Technology (Beverly, MA), and PARP-1 was from Santa Cruz Biotechnologies (Santa Cruz, CA). The alcohol dehydrogenase kit was from Diagnostic Chemicals Ltd.

Cortical Neurons Cultures

Primary cortical neuron cultures were prepared from embryonic day 16–17 rats as described earlier (Dutton, 1990; Ramachandran et al., 2003). The neurons were initially suspended in

MEM containing 10% HS and 10% FBS. From the initial media change onward, MEM with 10% HS was used. Cells were plated into six-well culture plates (1.2×10^6 cells/ well) previously coated with poly-D-lysine. For imaging studies, a lower seeding density of 5–6 $\times$ 10^5 cells/well was plated on 25-mm coverslips to allow for clear identification of neurons. On the following day, neurons were treated with mitotic inhibitors to prevent glial contamination. Cells were fully differentiated by day 5 in vitro and ready to use for the following experiments.

Ethanol Treatments

On the fifth day, neurons were treated with ethanol (4 mg/ml) for the duration mentioned in each experiment. An ethanol-filled beaker was placed in incubators to maintain optimum ethanol concentrations in the culture media at all times (Heitman et al., 1987; Devi et al., 1993). Media ethanol concentration was determined by using the alcohol dehydrogenase kit. To account for variations in baseline values within primary isolates and cultures, parallel controls were used with each duration of ethanol exposure.

In Vivo Model and Expression of Apoptosis

The in vivo exposure model was a postnatal rearing procedure (Diaz and Samson, 1980). Rat pups were artificially reared and administered ethanol (7.5% v/v, 5.6 g/kg/24 hr) or an isocaloric diet of maltose-dextrin (pair-fed control) during postnatal days 4 and 5. This exposure regimen was one that has previously been shown to elicit alterations in brain morphology (West, 1993). Blood ethanol levels 1.5 hr following the last dose of ethanol averaged 2.56 mg/ml $\pm$ 0.07 (SE; n = 50). These concentrations are clinically relevant and far below those that have produced extensive and likely nonphysiological measures of apoptotic death in vitro. This approach allows the animals to receive adequate nutrition even during periods of extreme intoxication. Briefly, polyethylene gastrostomy feeding tubes were implanted and formula was directly infused into the pup's stomach. Pups were reared in plastic cups floating in a temperature-controlled aquarium and were fed via flexible tubes connected to the cannula leading to the stomach. Formula was infused via syringes mounted to an automated infusion pump every 3 hr in 20-min fractions. The amount of formula supplied per day was equivalent to 33% of the mean body weight of the litter. Two hours after the last dose of ethanol or maltose-dextrin, pups were anesthetized, perfused intracardially with 0.9% saline, followed by fixation with 10% formalin. Brains were embedded in paraffin, 6-lm sections were cut, and two adjacent sections were stained for apoptosis.

In situ detection of apoptosis in the brain slices utilized the ApopTag reagent (Oncor, Gaithersburg, MD), which was used according to the manufacturer's directions wherein the newly generated 3′-H ends of fragmented DNA are stained. To quantify the extent of cell death, the NIH Image software package (v.1.55, Wayne Rasband, NIH) was used. The total numbers of cells and all immunopositive cells were determined in a 325- $\times$ 250-μm region with a Nikon Microphot-SA light microscope (Hamby-Mason et al., 1997). The extent of labeling was expressed as a percentage of positive cells. Sections were scanned for density and location of apoptotic cells in the following regions: neuroepithelium (NE) in the area just below the corpus callosum, dentate gyrus (DG), medial habenular nucleus (MHN), choroid plexus (CP), brainstem in the paramedian reticular nucleus, cerebellum (cerebellar granule cells), cortex (cortical layers 2–3), dorsomedial hypothalamus (DMH), and CA3 region of the hippocampus. These regions were selected as representative areas, with a total of five neonatal brains used for each analysis. As a positive control for each experiment, sections of rat mammary gland, whose cells undergo apoptosis during tissue regression following lactation, were stained simultaneously.

Measurement of Reactive Oxygen Species

Flow cytometry—Generation of reactive oxygen species (ROS) was estimated with the fluorescent probe DCF-DA as previously described (Kim et al., 2001; Rathinam et al., 2006). Cells were harvested and washed with phosphate-buffered saline (PBS) and resuspended in PBS at a concentration of 1×10^6 cells/ml. DCF-DA was added to a final concentration of 20 μM and incubated for 30 min at 378C. After incubation, the cells were washed with PBS and resuspended in PBS containing 1% BSA. ROS generation in 10,000 cells was measured with FACS (505 nm ex, 535 nm em) under FL-1.

Confocal microscopy—The initial onset of ROS generation was measured with a low-intensity argon laser, with 488 nm excitation and emission filtered with a 515–530-nm bandpass filter (Ramachandran et al., 2003). Briefly, fields were selected with four to six clearly identifiable cells. At the start of the experiment, 25 μM DCF-DA was added to the media and allowed to diffuse into the cells for 5 min. Prior to addition of ethanol, an initial scan was taken as time 0. After ethanol addition, ROS-mediated increases in DCF fluorescence intensity were determined by scans taken once every 5 min, typically for a 40-min period.

Measurement of Reduced Glutathione

The distribution of total cellular glutathione content was measured by flow cytometry and multiphoton microscopy using monochlorobimane (MCB), a nonfluorescent probe that is freely permeable across cell membranes. It conjugates with GSH by a glutathione-S-transferase-catalyzed reaction to form a highly fluorescent product.

Flow cytometry—Flow cytometry was utilized to estimate reduced glutathione in large populations of neurons (10,000 cells). At the end of ethanol regimens, neurons were labeled with 10 μM of MCB for 15 min. Cells were scraped from the plates, washed once, resuspended in cold PBS with 1% BSA, and immediately analyzed using FACS Aria.

Live cell imaging studies—Neurons plated on 25-mm coverslips were incubated with 4 mg/ml ethanol for various times. After treatment, cells were washed with phenol-free MEM supplemented with 20 mM HEPES and incubated with 50 μM MCB for 15 min at 37°C, washed again, and mounted on steel chambers in 1.5 ml medium. Cells were imaged immediately on a Zeiss LSM 510 microscope, with a × 63, 1.4 NA objective. MCB was excited at 800 nm using a multiphoton Ti-sapphire Mira 900 laser with a 5-W Verdi laser and the emission collected through a 565–615-nm barrier filter. The laser intensity output used was attenuated to minimize photobleaching and phototoxicity to the cells during scanning (3.94 sec). For reproducibility and comparison purposes, all experimental conditions as well as microscope settings were kept identical among all the experiments. Semi-quantitative analysis of mean fluorescence intensities of GSH-MCB was performed using built-in Zeiss software. Eight to ten images per sample were randomly obtained from each treatment group. In addition, data from three independent experiments was collected and used for analysis. In all, approximately 300 cells in each group were measured for their intensities. A region of interest was drawn around each neuron cell body and the average intensity measured. An intensity threshold was initially set and kept constant for all images analyzed, and the data are represented as mean arbitrary fluorescence intensity units (AU). To assess the subpopulation of neurons based on their GSH content, corresponding intensity ranges were set between the maximum and minimum threshold values. The distribution of cells falling in each category was counted. These numbers were then represented as percentage of the total number of cells in that particular treatment group.

Immunofluorescence Detection of Oxidative Stress and Apoptosis

Cells were grown in Nunc chambers and, after ethanol treatment, were labeled with MCB, washed, and fixed with 4% paraformaldehyde in PBS at room temperature. After blocking with blocking buffer (0.25% Triton, 2 g BSA, 4 ml goat serum, 4 g fish skin gelatin in 200 ml PBS) for 1 hr, the neurons were incubated with antibody against HNE (mouse monoclonal) for 1 hr. This was followed by several washes and labeling with secondary antibody conjugated with Alexa 633 for 1 hr. Cells were washed with PBS and images acquired using an Olympus FV500 confocal microscope under a × 40 oil immersion objective, NA 1.4, zoom 1.5. Fluorochromes were excited using a 405-nm (MCB) and a 633-nm HeNe laser (HNE protein adducts), and the detector slits were configured to minimize any cross-talk between the channels.

TUNEL Staining of Cultured Cortical Neurons

Neurons grown on coverslips were washed with PBS, fixed in 1% paraformaldehyde in PBS, and postfixed cells in precooled ethanol and acetic acid (ratio 2:1). Cells were incubated in equilibration buffer and TdT enzyme. Antidioxigenin fluorescein conjugate was added onto the coverslips, washed with PBS, and mounted using Vectashield with DAPI. Images were obtained using an Olympus B-Max fluorescence microscope (Olympus, Tokyo, Japan) and recorded in a Spot II digital camera (Diagnostic Instruments, Tokyo, Japan). For experiments with neurons pretreated with BSO and exposed to ethanol for 2 hr, in addition to TUNEL staining, cells were also labeled with propidium iodide (PI). PI penetrates all fixed cells and was used solely to count the total number of cells, whereas the TUNEL-positive cells indicated DNA damage. Under identical settings of Olympus FV-500, four different fields from each group were collected. The total number of cells per field stained with PI (red) was first counted. The number of cells with green fluorescence (TUNEL positive) could have been expressed as a percentage of the total number of cells, but there were marked fluorescence intensity variations between experimental samples. Therefore, the extent of damage within a given cell is best reflected when expressed in terms of fluorescent intensity rather than number of TUNEL-positive cells. The NIH ImageJ software was used for analysis of fluorescence intensity. The image threshold was set constant for all control and experimental images measured, at a range of 30–118. The intensity value obtained for each image was divided by the number of cells in each to reflect the average intensity/cell.

Cell Sorting Based on GSH Content and Subsequent Western Blot Analysis of HNE, Active Caspase-3, and PARP-1

Neurons cultured in 100-mm dishes were treated with ethanol (4.0 mg/ml) for 2 hr and stained with 10 μM MCB for 15 min. At the end of the incubation, cells were scraped; pooled from 10 plates; resuspended in culture media; and, based on their fluorescence intensities, sorted by FACSAria into low (lower 15%; ~3.76 × 10 cells)- and high (upper 15%; ~1.56 × 10 cells)-GSH populations. Samples from each population were pelleted and lysed in PARP buffer (62.5 mM Tris/HCl, pH 6.8, 6 M urea, 10% glycerol, 2% SDS, 0.00125% bromophenol blue, 5% β-mercaptoethanol), sonicated for 15 sec, and incubated at 65°C for 15 min. Proteins were separated on a 12.5% SDS gel and electrophoretically transferred onto PVDF (polytran) membrane followed by blocking with nonfat dry milk in TBST (50 mM Tris-HCl, pH 7.4, 150 mM NaCl, 0.2% Tween 20) for 1 hr. The membrane was incubated overnight with primary antibody: mouse monoclonal for HNE (1:200), rabbit polyclonal for caspase-3 (1:500), or rabbit polyclonal for PARP-1 (1:250). Tubulin was used as a loading control. The protein bands were detected with an ECL kit (Pierce, Rockford, IL).

GSH Depletion Method

To deplete neurons of GSH, cells were treated with BSO for 24 hr prior to ethanol exposure (4 mg/ml) for an additional 2 hr. Appropriate controls for each group were maintained and run simultaneously. Samples were lysed with RIPA buffer at 4°C and processed as described above.

Protein Determinations

Protein was estimated by the method of Bradford (1976), using a kit from Bio-Rad. BSA was utilized as the standard.

Statistical Analysis

Data are expressed as mean ± SEM. One-way analysis of variance followed by Students Newman Kuels test was used for comparisons between the control and the treated groups. In certain cases, multigroup comparisons were checked by using a Tukey WSD method. $P < 0.05$ was considered statistically significant. For GSH distribution in neurons (Fig. 4), factorial analysis of variance was performed between average intensities and time of ethanol exposure, using $P < 0.01$ as statistically significant.

RESULTS

Variable Apoptotic Responses to Ethanol: Cells in the Developing Brain

Prior studies have illustrated that the rodent brain is especially sensitive to ethanol-mediated apoptotic death during the early postnatal (PN) period (Heaton et al., 2002; Light et al., 2002). The data in Figure 1 were derived from an established in vivo postnatal rearing model in which pups were exposed to ethanol on PN days 4 and 5, a period of high ethanol vulnerability (West et al., 1984; West, 1993). Apoptotic indices utilizing ApoTag are expressed in nine "brain regions" on PN5, at which time blood ethanol levels were approximately 2.5 mg/ml. This method is a direct measure of DNA fragmentation associated with apoptosis. There are three key points to be made from these data (Fig. 1). First, there is a detectable baseline of cell death at this PN5 time point. Second, ethanol strikingly increases this measure of apoptosis. Third, although the ethanol-related increase is *relatively* high, e.g., two to five times above control values, the *net* increases are typically only seen in 3–6% of the total cells in a given field/area. Thus, in each of these images, only a small fraction of the cells are expressing enhanced apoptotic indices in response to ethanol, and this is a clear example of a variable sensitivity in an in vivo setting.

There was a significant ($P < 0.05$) increase in cell death in all tested brain regions of the ethanol-treated animals, compared with ad lib and pair-fed controls (Fig. 1). Between ad lib and pair-fed controls, the values are also quite similar, suggesting little if any influence of the isocaloric diet on the outcome measures. The following values, presented as the percentage of apoptotic cells/field, are those for the ad lib control, pair-fed control, and ethanol-treated groups, respectively. These regions include the neuroepithelium (3.5 ± 0.92 and 3.7 ± 0.51 vs. 7.6 ± 0.62) and choroid plexus (1.4 ± 0.93 and 1.32 ± 0.86 vs. 6.98 ± 2.46), cerebral cortex (1.3 ± 0.34 and 0.4 ± 0.27 vs. 6.9 ± 0.60), CA3 region of the hippocampus (1.8 ± 0.86 and 1.0 ± 0.43 vs. 4.825 ± 1.05), and dentate gyrus (1.8 ± 0.86 and 0.79 ± 0.25 vs. 9.27 ± 3.2), brainstem (1.5 ± 0.33 and 1.95 ± 0.76 vs. 9.12 ± 1.06), cerebellum (0.9 ± 0.30 and 0.783 ± 0.26 vs. 4.01 ± 0.97), dorsomedial hypothalamus (1.6 ± 0.38 and 2.06 ± 0.65 vs. 6.47 ± 1.36), and medial habenular nucleus (0.5 ± 0.5 and 0.90 ± 0.26 vs. 4.49 ± 0.48).

Selective Vulnerability of Cultured Cortical Neurons to Ethanol

Previous studies have illustrated that ethanol-mediated oxidative stress can play a causal role in apoptotic death of cultured fetal rat cortical neurons (Ramachandran et al., 2003). These experiments estimated timelines for the onset of ROS generation and apoptosis, as well as their mitigation by manipulation of GSH homeostasis. The data revealed a rapid, highly varied neuronal response to ethanol, but only in some cells, a setting similar to what was observed in in vivo exposure models (Fig. 1; Heaton et al., 2002; Light et al., 2002). The following experiments with cultured fetal rat cortical neurons demonstrate the variability of oxidative stress and apoptotic responses to ethanol, the large variations in baseline GSH content, and the connections between the latter and neuron survival responses to ethanol. They address one possible mechanism underlying the apparent selective vulnerability to ethanol-mediated oxidative stress and related apoptotic death.

Variability of Ethanol-Mediated ROS Production

The experiments presented in Figure 2 illustrate wide variations in oxidative stress responses in neurons following an ethanol challenge. The experimental approach utilized both confocal imaging and flow cytometry of much larger populations of cortical neurons. Figure 2A is an image of neurons that have been preloaded with DCF-DA, followed by an 18-min exposure to ethanol (4 mg/ml). There are seven clear cells in the field, each showing a varying degree of fluorescence increase within this short time. Background fluorescence intensities were normalized to near zero prior to ethanol addition, and parallel control experiments showed no increase in emissions in the absence of ethanol. The average fluorescence intensity per unit area was calculated for each cell and plotted in Figure 2B. The fluorescence units varied from about 1,200 in one cell to over 9,000 in another neuron. This is a typical pattern, but, because this is a small sample size, additional measures of ethanol-mediated oxidative stress utilized flow cytometry to confirm the wide distribution of responses in larger neuron populations (10,000 cells per estimate). With identical neuron cultures and DCF-DA as a probe, Figure 2C illustrates a typical flow cytometry scattergram of one experiment. It illustrates the range of fluorescence units, which varies by over a log power, and the ethanol-related increase in DCF fluorescence. The latter boost in ROS is illustrated in an enhanced P1 (percentage gated peak) from 53.9% (control) to 74% (ethanol), a 37% increase.

Variability of Ethanol-Mediated Increases in Neuron Apoptosis

Figure 3 illustrates an approach (TUNEL) comparable to that in the postnatal rearing model (Fig. 1) to estimate apoptosis in cultured neurons. Ethanol exposure was for 24 hr (4 mg/ml), a duration that has previously been shown to enhance apoptotic indices (including end point DNA fragmentation) in these cells (Ramachandran et al., 2003). Three typical fields are presented vertically, with the left panels showing TUNEL-stained neurons, the center panels showing DAPI nuclear stains to identify all cells present, and the right panels showing merges of the first two panels. Although multiple neurons are positive for TUNEL, there are seven arrows within the DAPI fields that flag neurons that do not express TUNEL staining. These TUNEL-negative neurons have normal nuclei, whereas the TUNEL-positive neurons are undergoing nuclear condensation. Thus, even with rigorous ethanol exposure, some neurons within this very pure preparation are resistant to ethanol-induced apoptosis. Over 95% of the cells in these cultures are MAP2 positive, and there are essentially no GFAP-positive cells in the fields (data not shown). Consequently, the resistant cells are not contaminating glia that contain high GSH.

Heterogeneity of Neuron GSH Content

The intent of the following experiments was to determine whether the above-described variations in neuron responses to ethanol are mediated by differences in neuron GSH content. That this could be the case is supported by prior evidence of GSH-related neuroprotection; widely varying GSH levels in cultured fetal cortical neurons (present studies); and a literature indicating that, in varied cell types, sensitivity to oxidative stress can be dictated by GSH content (Devesa et al., 1993; West et al., 2000). The heterogeneity of GSH content of cultured fetal cortical neurons is illustrated by multiphoton imaging and by flow cytometry experiments (Figs. 4, 5, respectively). Figure 4A is a representative panel of neurons preincubated with 50 μM MCB, followed by a 15-min exposure to ethanol (4 mg/ml). Typically, fluorescence is less for the ethanol-exposed cells (additionally shown in Fig. 5A from flow cytometry experiments), and there is an observable variation in fluorescence within cells in each field, hence varying GSH content. Figure 4B illustrates the large differences in neuron GSH content in populations of neurons that had been exposed to ethanol (4 mg/ml) for 15, 30, or 60 min. The graph shows the percentage of cells counted as a function of cellular GSH mean fluorescence intensity (arbitrary units). In addition to the wide variation in neuron GSH, there is a redistribution of GSH within 1 hr of ethanol treatment, with a shift of the peak of the curves to the lower GSH range. Around 300 cells were counted for each time point.

The panel of flow cytometry figures in Figure 5A emphasizes two features. They confirm the wide variability of GSH content in a large population (10,000 events) as well as a shift of GSH to the left (lower GSH content) following a 2-hr exposure to ethanol (4 mg/ml, 10,000 events) and/or BSO. Pretreatment of the neurons with 200 μM BSO clearly decreased GSH content, and the ethanol-related reduction is strikingly magnified by cotreatment with 200 μM BSO. This is also exemplified in the bar graph in Figure 5B, which is a composite of three experiments. Compared with controls, the ethanol-related decline was 23% ($P = 0.01$), BSO pretreatment achieved a 66% reduction in GSH content, whereas cotreatment with BSO and ethanol presented a 69% decline. The value for ethanol and BSO cotreatment was significantly less than for ethanol alone ($P < 0.05$), yet it did not exceed that for BSO alone ($P > 0.05$).

GSH Content Is an Important Determinant of Ethanol's Neurotoxicity

Previous studies have illustrated that normalizing or enhancing cultured cerebral cortical neuron GSH, either by administration of N-acetylcysteine or by coculturing with astrocytes, can prevent ethanol-mediated oxidative stress and subsequent apoptotic death (Ramachandran et al., 2003; Watts et al., 2005). The following experiments utilized the BSO pretreatment regimens. The effects of these manipulations on ethanol-related oxidative stress and apoptosis are illustrated below.

Oxidative stress—As shown in Figure 6, a 2-hr exposure to ethanol (4 mg/ml) increased ROS generation (by 46% in this experiment, $P < 0.05$). In the absence of ethanol, depleting neurons of GSH for 24 hr with BSO alone likewise increased ROS content by 60% ($P < 0.05\%$). Prior depletion of neuron GSH clearly exacerbated the response to ethanol, increasing ROS determinants by 115% at 2 hr of exposure ($P = 0.02$, ethanol alone vs. ethanol plus BSO).

Apoptosis—Cortical neurons exhibit significant increases in DNA fragmentation and annexin V surface binding in response to ethanol by 12 hr of exposure, at the earliest (Ramachandran et al., 2003; Watts et al., 2005). In the present study, we assessed ethanol-related changes in apoptosis-related DNA damage at earlier time points in the presence or absence of GSH depletion (Fig. 7). As shown here, pretreatment with BSO alone for 24 hr, a

maneuver that depleted GSH by over 65%, or ethanol exposure alone for 2 hr increased TUNEL-positive responses (69.11% ± 2.82% or 63.42% ± 3.40%, respectively) compared with the controls (38.42% ± 1.32%, $P < 0.05$). Treatment of GSH-depleted cells with ethanol (4 mg/ml, 2 hr) further increased this measure of DNA damage by 111% ± 8.7% ($P = 0.001$, compared with control or ethanol alone).

Ethanol Responses in High- and Low-GSH Populations

Cell sorting was used to isolate high- and low-GSH neurons. Oxidative damage and early apoptosis responses to ethanol in neurons representing those with the lower 15% of GSH content vs. those containing the upper 15% were determined. Neurons were treated with ethanol (4 mg/ml, 2 hr), after which they were harvested and sorted into low- and high-GSH populations by FACSAria. Examples of the typical GSH distributions can be seen in Figure 5A.

Oxidative damage—As an estimate of oxidative damage, lysates of the two neuron populations were tested for expression of 4-hydroxynonenal (HNE) adducts. Previous studies in our laboratory found increased HNE-protein adducts in mitochondria of fetal brains exposed to ethanol in utero (Ramachandran et al., 2001) and in cultured fetal cortical neurons within 1 hr of ethanol treatment (Ramachandran et al., 2003). Figure 8A is a confocal image of neurons (not sorted) exposed to ethanol and costained for GSH (monochlorobimane) and HNE adducts, illustrating a typical pattern in which neurons staining the least for GSH (green) most highly express HNE adducts (red) in response to an ethanol challenge (4 mg/ml, 2 hr). The Western blots shown in Figure 8B were derived from ethanol-challenged neurons (4 mg/ml, 2 hr) that had subsequently been sorted into high- and low-GSH content. There was a 60% higher expression of HNE adducts in the low-GSH population compared with the high-GSH neurons.

Apoptosis—Expression of two early apoptosis-related markers, active caspase-3 and the 24-kDa PARP-1 fragment, were determined in both low- and high-GSH populations of ethanol-exposed (4 mg/ml, 2 hr) neurons. Figure 9A illustrates that, in the low-GSH neurons, active caspase-3 (11 kDa) was 36% higher than in the high-GSH cells, whereas procaspase-3 expression was 155% higher in the high-GSH population. The 24-kDa PARP-1 fragment was likewise 37% higher in the low-GSH neurons (Fig. 9A). A second series of experiments depicted in Figure 9B, demonstrates a comparable effect in neurons exposed to ethanol after GSH depletion. These experiments did not utilize cell sorting. Cultured neurons were pretreated with BSO for 24 hr prior to ethanol exposure (4 mg/ml, 2 hr). Western blot analysis for active caspase fragment expression demonstrates an increase of 51% in cells exposed to ethanol. This response was further exacerbated when GSH was depleted by BSO pretreatment, which generated a 160% increase in active caspase expression compared with controls. These data demonstrate that ethanol-mediated early apoptosis measures are preferentially active in neurons with low endogenous GSH content and in neurons in which GSH has been artificially depleted.

DISCUSSION

There is extensive evidence that ethanol can affect the number of neurons in multiple regions of the developing brain and that this can result in decreased progenitor cell proliferation, neuron migration, and death of postmitotic neurons (West et al., 1984; Miller and Kuhn, 1995; Olney et al., 2001; Farber et al., 2005; Young and Olney, 2006). Additionally, the demise of neurons that is connected to ethanol exposure reflects increased apoptotic death (West et al., 1984; de la Monte et al., 2001; Mooney and Miller, 2001; Ramachandran et al., 2001, 2003; Olney et al., 2002; Heaton et al., 2003). One central theme

in the composite of these reports is that ethanol-related death does not occur in a massive manner with large populations of neurons dying except with very high, nonclinically relevant levels of ethanol. Rather, there are modest increases in neuron demise, the degree of which likely depends on stages of development and brain region affected as well as the severity of ethanol exposure. A key unanswered question is: within an apparently homogeneous population, why do some neurons die while many neurons survive the same ethanol insult? Understanding the mechanism underlying this resistance/sensitivity phenomenon is central to developing interventions for this toxic response to ethanol.

Selective Vulnerability of Neurons to Ethanol

Selective vulnerability is a toxicological reality that reflects a heterogeneity of responses to a stressor, often within cells of a highly homogenous population (Castoldi et al., 2001; Whetsell, 2002). In short, some cells respond strongly to a stressor (highly vulnerable), whereas others may not be affected at all, under identical conditions. That this occurs in the developing brain in vivo, in response to ethanol, has been reported by others (Young and Olney, 2006) and is illustrated in Figure 1. The latter documents the ethanol-related increase in brain cell apoptosis in multiple regions while exemplifying that this substantial fractional increase occurs in relatively few cells at a given time point. Over time, with repeated insults, the accumulated neuron loss likely produces functional consequences (Young and Olney, 2006). The postnatal rearing model utilized in Figure 1 generated blood alcohol levels in excess of 2 mg/ml but less than 3 mg/ml. These are clinically relevant levels that were administered in a "binge" pattern. This is a consumption pattern in women who drink while pregnant (Stephens, 1985), and the blood alcohol levels are consistent with those previously shown to elicit neuron apoptotic death at this stage of development in rodent models (West, 1993; Siler-Marsiglio et al., 2005).

Studies in our laboratory have utilized quite pure (>95%) primary cultures of fetal rat cortical neurons to address mechanisms of ethanol-mediated toxicities, and clear evidence of varying sensitivities to ethanol was apparent, although the issue was not addressed (Ramachandran et al., 2003). These studies provided evidence that ethanol-related apoptotic death of neurons can be mediated by a very rapid onset of increased ROS production. These two measures, increased ROS and apoptosis, were observed to vary widely among the cortical neurons, even with a fixed ethanol concentration and duration of exposure. Figure 2A,B exemplifies the striking variation in the ROS response, generated within minutes of exposure to a fairly high ethanol level (4 mg/ ml). Prior studies have documented a maximal response within 30 min (Ramachandran et al., 2003). In the microscopic image (Fig. 2A), arbitrary fluorescence unit intensities differed by over seven times within the captured cell population. This is typical. Flow cytometry measurements in large neuron populations confirmed this (Fig. 2C). TUNEL/DAPI cotags in Figure 3, obtained with neurons exposed to an ethanol regimen clearly illustrate that some neurons survived whereas others undergo apoptosis. This is a phenomenon previously observed via flow cytometry in much larger populations (Watts et al., 2005; Rathinam et al., 2006). In summary, there is a striking variation in the very rapid prooxidant response to ethanol, which may ultimately translate into similar differences in onset of apoptotic death. One possible underlying mechanism could be heterogeneity of GSH homeostasis, a setting that is subject to external manipulation.

Variations in Neuron GSH Content as a Determinant of Neuron Sensitivity to Ethanol

Prior studies in our laboratory have utilized two approaches to normalize cultured cortical neuron GSH homeostasis, N-acetylcysteine treatment and coculturing with astrocytes. Both procedures prevented ethanol-mediated oxidative stress and subsequent apoptotic death in vitro (Ramachandran et al., 2003; Watts et al., 2005). Assays for total neuron GSH in these

and other studies illustrated substantial variations in cell GSH content, thus raising the possibility that it was a low-GSH subpopulation of neurons that expressed the high vulnerability to ethanol-related death. Reduction of cellular GSH levels has often been connected with increased sensitivity to toxicants (West et al., 2000; Wu and Cederbaum, 2001; Reed, 2004). With respect to a role for GSH and ethanol-related toxicity, the majority of the literature focuses on the liver, and there is evidence that GSH depletion can enhance an apoptotic response to CYP2E1-mediated oxidative stress in this organ (Wu and Cederbaum, 2001). In fetal cortical neurons, the setting is different, CYP2E being only slightly expressed, at most, and the source of the ethanol-related ROS increase being undetermined. However, the experiments illustrated in Figures 6 and 7 likewise show that prior depletion of GSH with BSO pretreatment further enhances ethanol-mediated ROS production and the apoptotic response (Figs. 7, 9). They support the concepts that ethanol-mediated oxidative stress is a key player in this apoptotic death process and that the latter could be mechanistically connected to neuron GSH homeostasis.

Oddly, there is a lack of literature addressing the concept that subpopulations of specific cells that normally possess low GSH content are predisposed to cytotoxicant damage. In nonneural cells, heterogeneity of GSH distribution in thymocytes can connect to sensitivity to apoptosis (Voehringer et al., 1998), and chemotherapeutic drug resistance can likewise be related to intracellular glutathione heterogeneity in murine leukemia (Tagliabue et al., 1993) and sarcoma cell lines (Richardson and Siemann, 1997). One of the most definitive studies of a heterogeneous content of GSH mediating toxicant responses utilized alveolar Clara cells in which GSH varies fourfold within the controls (West et al., 2000). It appears that these cells exist in subpopulations containing distinct GSH pools and that this cell-to-cell heterogeneity of GSH closely correlates with sensitivity to toxicant injury. With respect to brain cells, there is little information on GSH distribution in specific neuron populations, and we are aware of no documented connections between cortical neuron GSH heterogeneity and sensitivity to ethanol. One potentially important issue that we have not addressed in the experiments described above is the relevance of mitochondrial GSH content. The ethanol literature is somewhat controversial with respect to effects of mitochondrial GSH on the cellular or organ (mostly hepatocyte or liver) GSH (Reed, 2004). However, there is some persuasive literature suggesting that, at least in the liver, variations or changes in mitochondrial, rather than cytosolic, GSH are the primary determinants of toxic responses to ethanol (Fernandez-Checa et al., 1998; Hoek et al., 2002). In the present studies with neurons, total cellular GSH content, most of which is cytosolic, does indeed appear to dictate oxidative stress and apoptotic responses to ethanol. However, mitochondrial GSH could be concomitantly reduced, and this might be a highly relevant factor. Future studies will address this.

Heterogeneity of GSH Homeostasis May Determine Neuron Sensitivity to Ethanol-Mediated Apoptosis

Cell sorting experiments further suggest a connection between neuron susceptibility to ethanol-mediated apoptosis and GSH content. Rarely have we observed that more than 10–15% of cultured neurons (often less) express activated apoptotic pathways in response to ethanol at concentrations up to 4 mg/ml (Ramachandran et al., 2003; Watts et al., 2005; Fig. 1). This could reflect a setting in which a relatively small population of neurons expressing low GSH content is primarily responding to ethanol. Cell sorting of cultured neurons exposed to ethanol (2 hr, 4 mg/ml), which represented the lower 15% or the upper 15% of GSH content, was selected for the experiments depicted in Figures 8 and 9a. The end point measures selected in these cells were HNE adducts as a stable indicator of lipid peroxidation (also a proapoptotic toxin) and two markers of activation of apoptosis, activated caspase-3 and the 24-kDa PARP fragment. In these studies, differences between the two neuron

populations were clear, with the low-GSH population exhibiting higher active caspase-3, 24-kDa PARP-1, and HNE adducts in response to ethanol. This is supported by the GSH depletion experiments in which this maneuver elicited exaggerated oxidative stress and apoptotic responses to ethanol. Control neurons when sorted did not show any difference in these markers (data not shown).

In summary, these studies illustrate that there is a substantial heterogeneity in GSH content within cultured cortical neurons and that this may dictate their susceptibility to ethanol-mediated apoptotic death. They further demonstrate the central role of oxidative stress in this response and suggest future intervention approaches.

Acknowledgments

REFERENCES

Barnes DE, Walker DW. Prenatal ethanol exposure permanently reduces the number of pyramidal neurons in rat hippocampus. Brain Res. 1981; 227:333–340. [PubMed: 7260643]

Bearer CF, Swick AR, O'Riordan MA, Cheng G. Ethanol inhibits L1-mediated neurite outgrowth in postnatal rat cerebellar granule cells. J Biol Chem. 1999; 274:13264–13270. [PubMed: 10224086]

Castoldi AF, Coccini T, Ceccatelli S, Manzo L. Neurotoxicity and molecular effects of methylmercury. Brain Res Bull. 2001; 55:197–203. [PubMed: 11470315]

Chandler LJ, Sutton G, Norwood D, Sumners C, Crews FT. Chronic ethanol increases N-methyl-D-aspartate-stimulated nitric oxide formation but not receptor density in cultured cortical neurons. Mol Pharmacol. 1997; 51:733–740. [PubMed: 9145911]

Chen WJ, Maier SE, Parnell SE, West JR. Alcohol and the developing brain: neuroanatomical studies. Alcohol Res Health. 2003; 27:174–180. [PubMed: 15303628]

Crews FT, Waage HG, Wilkie MB, Lauder JM. Ethanol pretreatment enhances NMDA excitotoxicity in biogenic amine neurons: protection by brain derived neurotrophic factor. Alcohol Clin Exp Res. 1999; 23:1834–1842. [PubMed: 10591601]

de la, Monte SM.; Neely, TR.; Cannon, J.; Wands, JR. Ethanol impairs insulin-stimulated mitochondrial function in cerebellar granule neurons. Cell Mol Life Sci. 2001; 58:1950–1960. [PubMed: 11766890]

Devesa A, O'Connor JE, Garcia C, Puertes IR, Vina JR. Glutathi-one metabolism in primary astrocyte cultures: flow cytometric evidence of heterogeneous distribution of GSH content. Brain Res. 1993; 618:181–189. [PubMed: 8374750]

Devi BG, Henderson GI, Frosto TA, Schenker S. Effect of ethanol on rat fetal hepatocytes: studies on cell replication, lipid peroxidation and glutathione. Hepatology. 1993; 18:648–659. [PubMed: 8359806]

Diaz J, Samson HH. Impaired brain growth in neonatal rats exposed to ethanol. Science. 1980; 208:751–753. [PubMed: 7189297]

Dutton GR. Isolation, culture and the use of viable CNS perikarya. Methods Neurosci. 1990; 2:87–102.

Farber NB, Young C, Qin Y, Olney J. Susceptibility of non-human primate to ethanol-induced developmental neuroapoptosis. Program No. 916.5.2005. Society for Neuroscience. 2005 online Abstract Viewer/Itinerary Planner.

Fernandez-Checa JC, Garcia-Ruiz C, Colell A, Morales A, Mari M, Miranda M, Ardite E. Oxidative stress: role of mitochondria and protection by glutathione. Biofactors. 1998; 8:7–11. [PubMed: 9699001]

Goodlett CR, Thomas JD, West JR. Long-term deficits in cerebellar growth and rotarod performance of rats following "binge-like" alcohol exposure during the neonatal brain growth spurt. Neurotoxicol Teratol. 1991; 13:69–74. [PubMed: 2046629]

Gressens P, Lammens M, Picard JJ, Evrard P. Ethanol-induced disturbances of gliogenesis and neuronogenesis in the developing murine brain: an in vitro and in vivo immunohistochemical and ultrastructural study. Alcohol Alcoholism. 1992; 27:219–226. [PubMed: 1449557]

Hamby-Mason R, Chen JJ, Schenker S, Perez A, Henderson GI. Catalase mediates acetaldehyde formation from ethanol in fetal and neonatal rat brain. Alcohol Clin Exp Res. 1997; 21:1063–1072. [PubMed: 9309319]

He J, Nixon K, Shetty AK, Crews FT. Chronic alcohol exposure reduces hippocampal neurogenesis and dendritic growth of newborn neurons. Eur J Neurosci. 2005; 21:2711–2720. [PubMed: 15926919]

Heaton MB, Paiva M, Mayer J, Miller R. Ethanol-mediated generation of reactive oxygen species in developing rat cerebellum. Neuro-sci Lett. 2002; 334:83–86.

Heaton MB, Paiva M, Madorsky I, Shaw G. Ethanol effects on neonatal rat cortex: comparative analyses of neurotrophic factors, apoptosis-related proteins, and oxidative processes during vulnerable and resistant periods. Brain Res Dev Brain Res. 2003; 145:249–262.

Heitman DW, Frosto TA, Schenker S, Henderson GI. Stimulatory effects of ethanol on amino acid transport by rat fetal hepatocytes. Hepatology. 1987; 7:307–314. [PubMed: 3557310]

Hoek JB, Cahill A, Pastorino JG. Alcohol and mitochondria: a dysfunctional relationship. Gastroenterology. 2002; 122:2049–2063. [PubMed: 12055609]

Ikonomidou C, Bittigau P, Ishimaru MJ, Wozniak DF, Koch C, Genz K, Price MT, Stefovska V, Horster F, Tenkova T, Dikranian K, Olney JW. Ethanol-induced apoptotic neurodegeneration and fetal alcohol syndrome. Science. 2000; 287:1056–1060. [PubMed: 10669420]

Jacobs JS, Miller MW. Proliferation and death of cultured fetal neocortical neurons: effects of ethanol on the dynamics of cell growth. J Neurocytol. 2001; 30:391–401. [PubMed: 11951050]

Kim T, Jung U, Cho DY, Chung AS. Se-methylselenocysteine induces apoptosis through caspase activation in HL-60 cells. Carcinogenesis. 2001; 22:559–565. [PubMed: 11285189]

Light KE, Belcher SM, Pierce DR. Time course and manner of Purkinje neuron death following a single ethanol exposure on postnatal day 4 in the developing rat. Neuroscience. 2002; 114:327–337. [PubMed: 12204202]

Luo J, West JR, Pantazis NJ. Nerve growth factor and basic fibro-blast growth factor protect rat cerebellar granule cells in culture against ethanol-induced cell death. Alcohol Clin Exp Res. 1997; 21:1108–1120. [PubMed: 9309325]

Maier SE, West JR. Regional differences in cell loss associated with binge-like alcohol exposure during the first two trimesters equivalent in the rat. Alcohol. 2001; 23:49–57. [PubMed: 11282452]

Mattson SN, Riley EP. A review of the neurobehavioral deficits in children with fetal alcohol syndrome or prenatal exposure to alcohol. Alcohol Clin Exp Res. 1998; 22:279–294. [PubMed: 9581631]

Miller MW. Limited ethanol exposure selectively alters the proliferation of precursor cells in the cerebral cortex. Alcohol Clin Exp Res. 1996; 20:139–143. [PubMed: 8651443]

Miller MW, Kuhn PE. Cell cycle kinetics in fetal rat cerebral cortex: effects of prenatal treatment with ethanol assessed by a cumulative labeling technique with flow cytometry. Alcohol Clin Exp Res. 1995; 19:233–237. [PubMed: 7771654]

Miller MW, Potempa G. Numbers of neurons and glia in mature rat somatosensory cortex: effects of prenatal exposure to ethanol. J Comp Neurol. 1990; 293:92–102. [PubMed: 2312794]

Mooney SM, Miller MW. Effects of prenatal exposure to ethanol on the expression of bcl-2, bax and caspase 3 in the developing rat cerebral cortex and thalamus. Brain Res. 2001; 911:71–81. [PubMed: 11489446]

Moore DB, Walker DW, Heaton MB. Neonatal ethanol exposure alters bcl-2 family mRNA levels in the rat cerebellar vermis. Alcohol Clin Exp Res. 1999; 23:1251–1261. [PubMed: 10443994]

Olney JW, Wozniak DF, Jevtovic-Todorovic V, Ikonomidou C. Glutamate signaling and the fetal alcohol syndrome. Ment Retard Dev Disabil Res Rev. 2001; 7:267–275. [PubMed: 11754521]

Olney JW, Wozniak DF, Farber NB, Jevtovic-Todorovic V, Bittigau P, Ikonomidou C. The enigma of fetal alcohol neurotoxicity. Ann Med. 2002; 34:109–119. [PubMed: 12108574]

Ramachandran V, Perez A, Chen J, Senthil D, Schenker S, Henderson GI. In utero ethanol exposure causes mitochondrial dysfunction, which can result in apoptotic cell death in fetal brain: a potential role for 4-hydroxynonenal. Alcohol Clin Exp Res. 2001; 25:862–871. [PubMed: 11410723]

Ramachandran V, Watts LT, Maffi SK, Chen J, Schenker S, Henderson G. Ethanol-induced oxidative stress precedes mitochondrially mediated apoptotic death of cultured fetal cortical neurons. J Neurosci Res. 2003; 74:577–588. [PubMed: 14598302]

Rathinam ML, Watts LT, Stark AA, Mahimainathan L, Stewart J, Schenker S, Henderson GI. Astrocyte control of fetal cortical neuron glutathione homeostasis: up-regulation by ethanol. J Neurochem. 2006; 96:1289–1300. [PubMed: 16464233]

Reed DJ. Mitochondrial glutathione and chemically induced stress including ethanol. Drug Metab Rev. 2004; 36:569–582. [PubMed: 15554236]

Richardson ME, Siemann DW. Tumor cell heterogeneity: impact on mechanisms of therapeutic drug resistance. Int J Radiat Oncol Biol Phys. 1997; 39:789–795. [PubMed: 9369124]

Sastry PS, Rao KS. Apoptosis and the nervous system. J Neurochem. 2000; 74:1–20. [PubMed: 10617101]

Siler-Marsiglio KI, Paiva M, Madorsky I, Pan Q, Shaw G, Heaton MB. Functional mechanisms of apoptosis-related proteins in neonatal rat cerebellum are differentially influenced by ethanol at postnatal days 4 and 7. J Neurosci Res. 2005; 81:632–643. [PubMed: 16035105]

Sokol RJ, Delaney-Black V, Nordstrom B. Fetal alcohol spectrum disorder. JAMA. 2003; 290:2996–2999. [PubMed: 14665662]

Stephens CJ. Alcohol consumption during pregnancy among Southern city women. Drug Alcohol Depend. 1985; 16:19–29. [PubMed: 4064908]

Streissguth, AP. Fetal alcohol syndrome. Baltimore: Paul H. Brookes Publishing Co; 1997.

Tagliabue G, Pifferi A, Balconi G, Mascellani E, Geroni C, D'Incalci M, Ubezio P. Intracellular glutathione heterogeneity in L1210 murine leukemia sublines made resistant to DNA-interacting anti-neoplastic agents. Int J Cancer. 1993; 54:435–442. [PubMed: 8509218]

Voehringer DW, McConkey DJ, McDonnell TJ, Brisbay S, Meyn RE. Bcl-2 expression causes redistribution of glutathione to the nucleus. Proc Natl Acad Sci U S A. 1998; 95:2956–2960. [PubMed: 9501197]

Watts LT, Rathinam ML, Schenker S, Henderson GI. Astrocytes protect neurons from ethanol-induced oxidative stress and apoptotic death. J Neurosci Res. 2005; 80:655–666. [PubMed: 15880562]

West JA, Chichester CH, Buckpitt AR, Tyler NK, Brennan P, Helton C, Plopper CG. Heterogeneity of clara cell glutathione. A possible basis for differences in cellular responses to pulmonary cytotoxicants. Am J Respir Cell Mol Biol. 2000; 23:27–36. [PubMed: 10873150]

West JR. Use of pup in a cup model to study brain development. J Nutr. 1993; 123(Suppl 2):382–385. [PubMed: 8429390]

West JR, Dewey SL, Pierce DR, Black AC Jr. Prenatal and early postnatal exposure to ethanol permanently alters the rat hippocampus. Ciba Found Symp. 1984; 105:8–25. [PubMed: 6563993]

West JR, Goodlett CR, Bonthius DJ, Hamre KM, Marcussen BL. Cell population depletion associated with fetal alcohol brain damage: mechanisms of BAC-dependent cell loss. Alcohol Clin Exp Res. 1990; 14:813–818. [PubMed: 2088116]

Whetsell WO Jr. The mammalian striatum and neurotoxic injury. Brain Pathol. 2002; 12:482–487. [PubMed: 12408235]

Wu D, Cederbaum AI. Removal of glutathione produces apoptosis and necrosis in HepG2 cells overexpressing CYP2E1. Alcohol Clin Exp Res. 2001; 25:619–628. [PubMed: 11329505]

Young C, Olney JW. Neuroapoptosis in the infant mouse brain triggered by a transient small increase in blood alcohol concentration. Neurobiol Dis. 2006; 22:548–554. [PubMed: 16459096]

Young C, Klocke BJ, Tenkova T, Choi J, Labruyere J, Qin YQ, Holtzman DM, Roth KA, Olney JW. Ethanol-induced neuronal apoptosis in vivo requires BAX in the developing mouse brain. Cell Death Differ. 2003; 10:1148–1155. [PubMed: 14502238]

Young C, Roth KA, Klocke BJ, West T, Holtzman DM, Labruyere J, Qin YQ, Dikranian K, Olney JW. Role of caspase-3 in ethanol-induced developmental neurodegeneration. Neurobiol Dis. 2005; 20:608–614. [PubMed: 15927478]
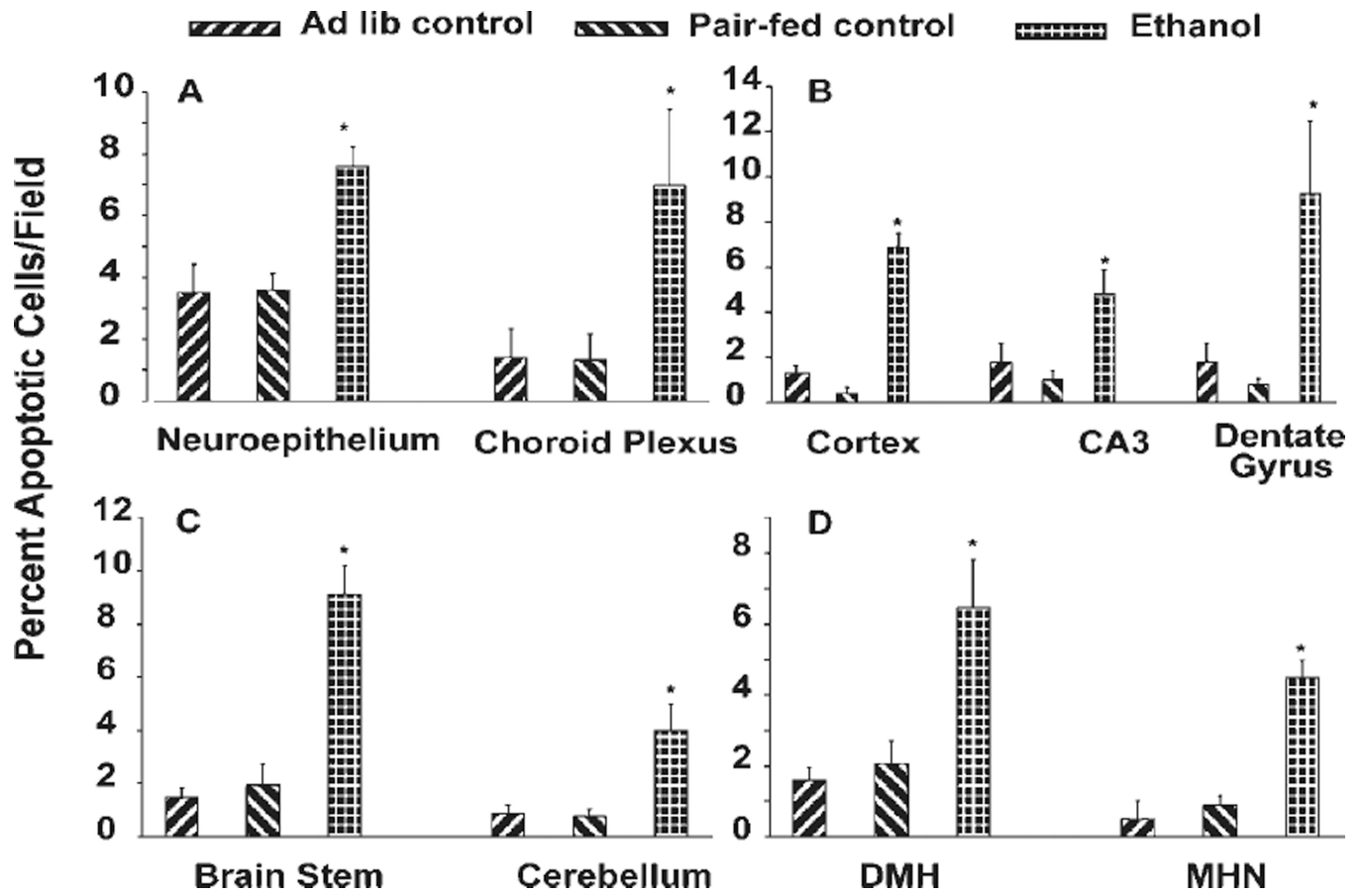
Fig. 1.
Variable apoptotic responses to ethanol in the intact developing brain. A postnatal rearing model was utilized for comparisons of the percentage of apoptotic cells from controls (ad lib suckle control and isocaloric maltose-dextrin pair-fed control) and ethanol (5.6 g/kg/24 hr on postnatal days 4 and 5) in neuroepithelium (**A**; left) and choroid plexus (right), layers 2–3 of the cortex (**B**; left), CA3 region of the hippocampus (center) and dentate gyrus (right), brainstem (**C**; left) and cerebellum (right), dorsomedial hypothalamus (DMH; **D**) and medial habenular nucleus (MHN). Bars represent the means ± SEM. *Statistically significant difference from both controls ($P < 0.05$).
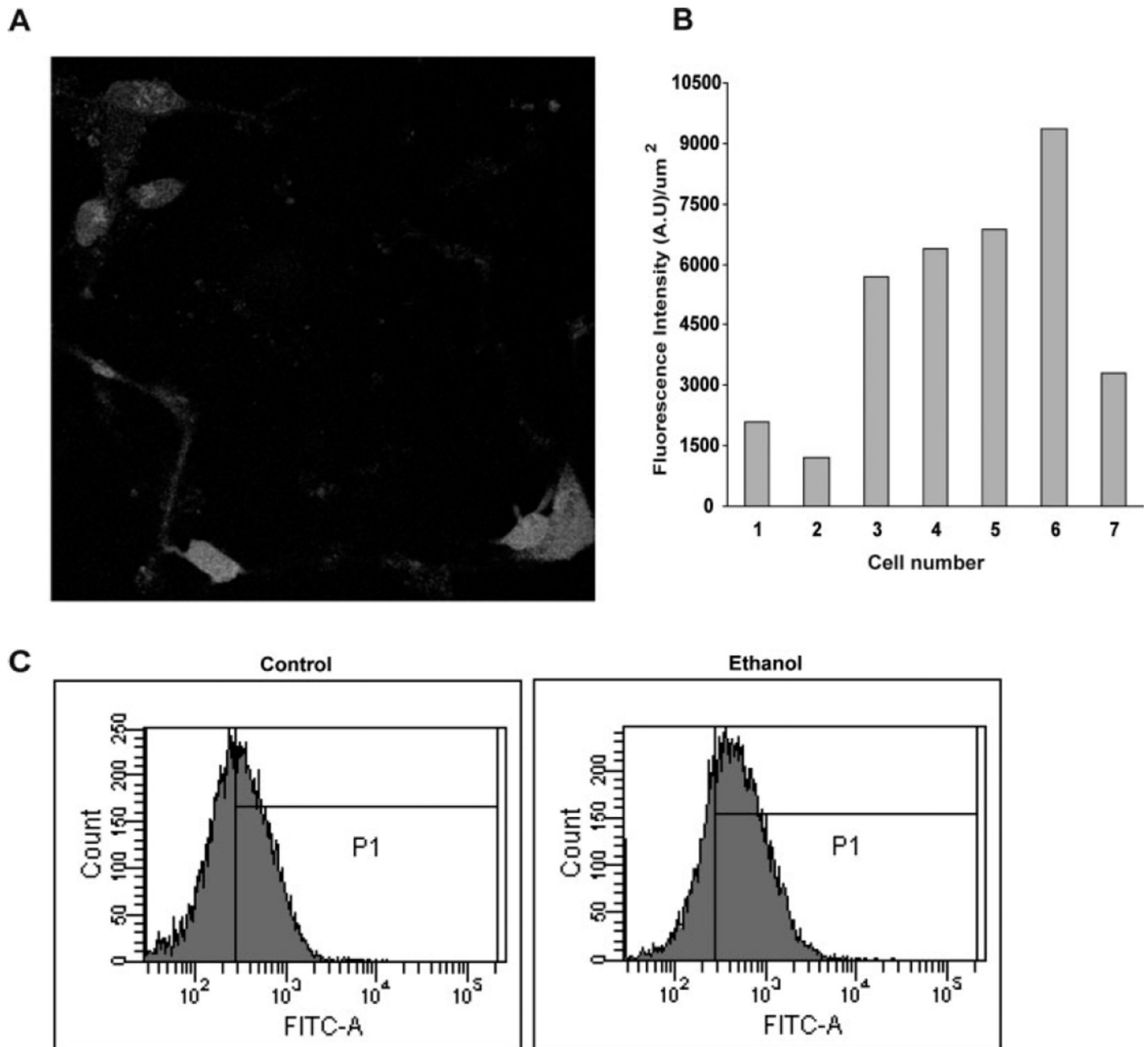
Fig. 2.
Variability of ethanol-mediated oxidative stress in cultured fetal cortical neurons. Live neurons plated on coverslips were preloaded with DCF-DA and treated with ethanol (4 mg/ml). **A**: A representative confocal microscopy image collected at 18.3 min after ethanol exposure shows a wide variability in DCF fluorescence. **B**: This variability is represented in a bar graph format. The average fluorescence intensity per unit area was calculated for each of the seven cells and plotted, and a sixfold variation between the brightest and the faintest stained cell can be observed. **C**: This variability is illustrated in large populations (10,000 events) of neurons by flow cytometry. There was a broad range in intracellular ROS generation and the ROS content shifted in a positive direction with ethanol treatment (4 mg/ml, 2 hr).
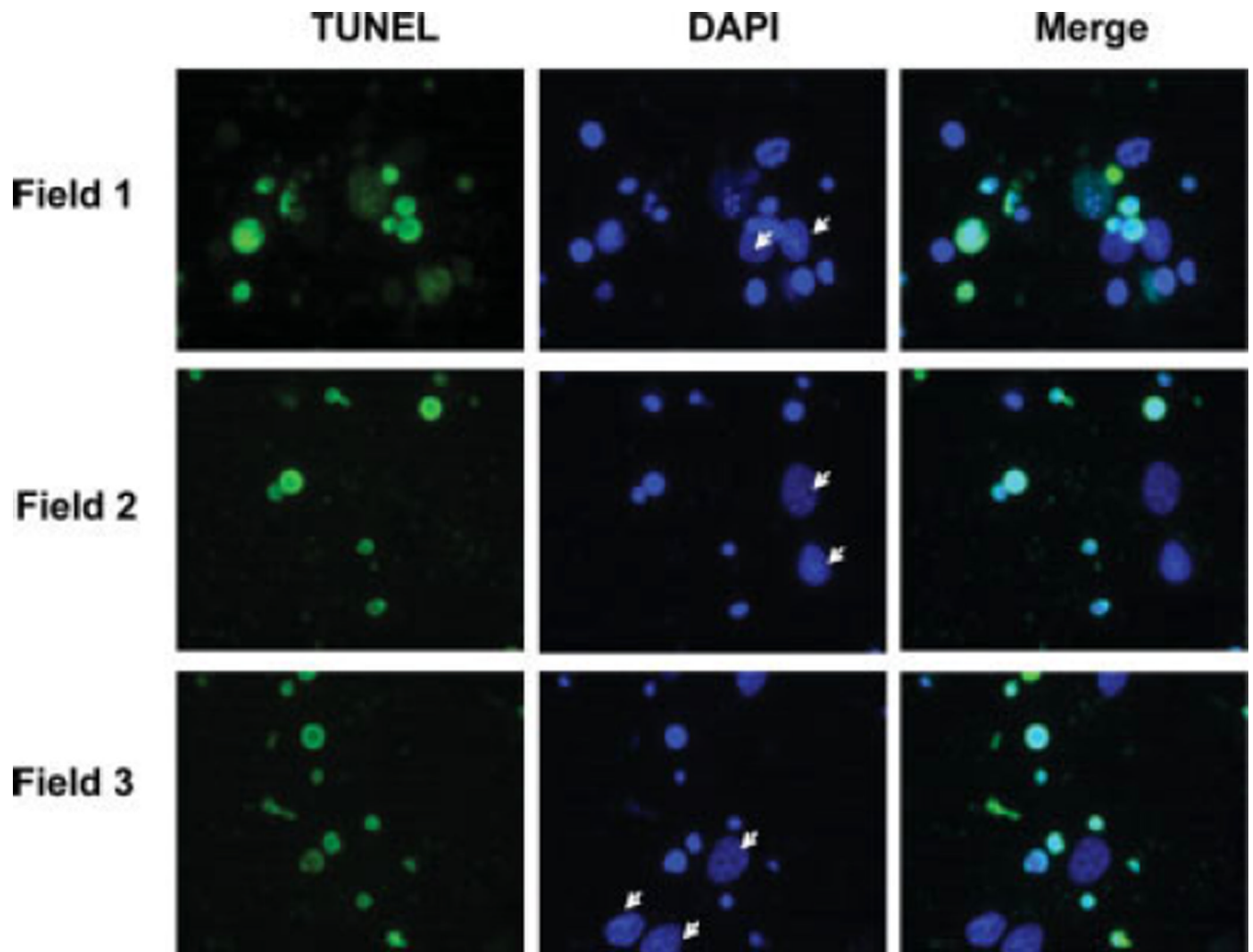
Fig. 3.
Variability of apoptotic response to ethanol in cultured fetal cortical neurons. Apoptosis-related effects of ethanol on neuronal DNA in three random fields. Cells were treated with 4 mg/ml ethanol for 24 hr and assessed for DNA damage with the TUNEL assay as seen by FITC (green) stain. Cells were counterstained with DAPI (blue) to label all nuclei. Not all nuclei, as visualized by DAPI, showed TUNEL staining. The arrows in the middle column identify cells that are healthy, not susceptible to ethanol treatment, and do not colocalize with TUNEL staining as illustrated in the third column (merge).
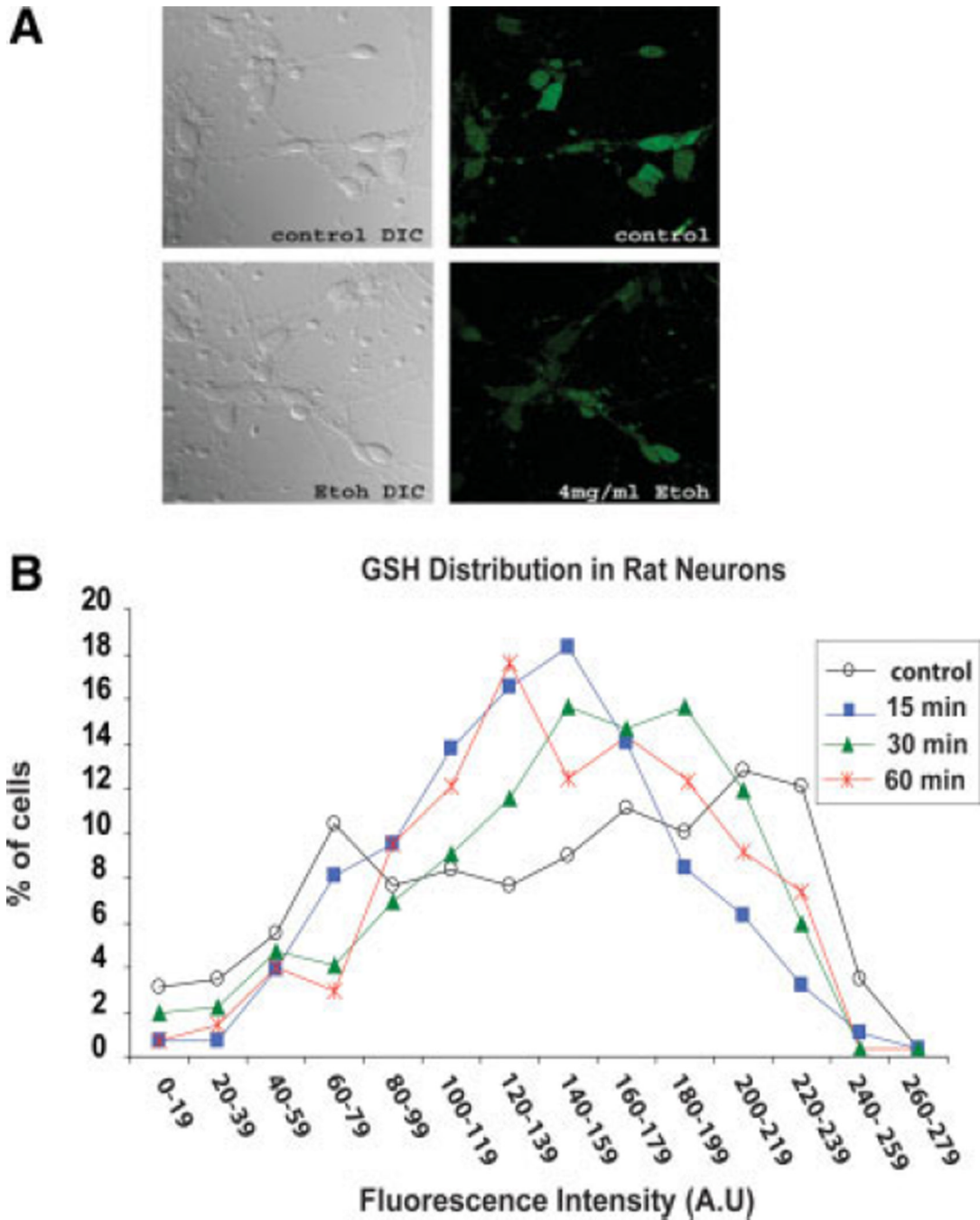
Fig. 4.
Heterogeneity of GSH content in cultured fetal cortical neurons. Neurons grown on
coverslips were treated with ethanol (4 mg/ ml) for various times and labeled with 50 μM
MCB (a GSH-sensing probe) for the final 15 min of incubation. **A:** Random images across
the coverslips were collected using a multiphoton microscope. Representative images show
the random distribution of GSH-related fluorescence among the neurons in control and in
ethanol-treated neurons (15-min exposure). **B:** The graph shows the percentage of cells
counted as a function of cellular GSH mean fluorescence intensity (arbitrary units). With
ethanol treatment, a decrease in fluorescence (GSH) is observed along with transient
redistribution of GSH at three early time points. The total number of cells in each group was

as follows: control (n = 289) and ethanol exposure for 15 min (n = 284), 30 min (n = 321), and 60 min (n = 272).
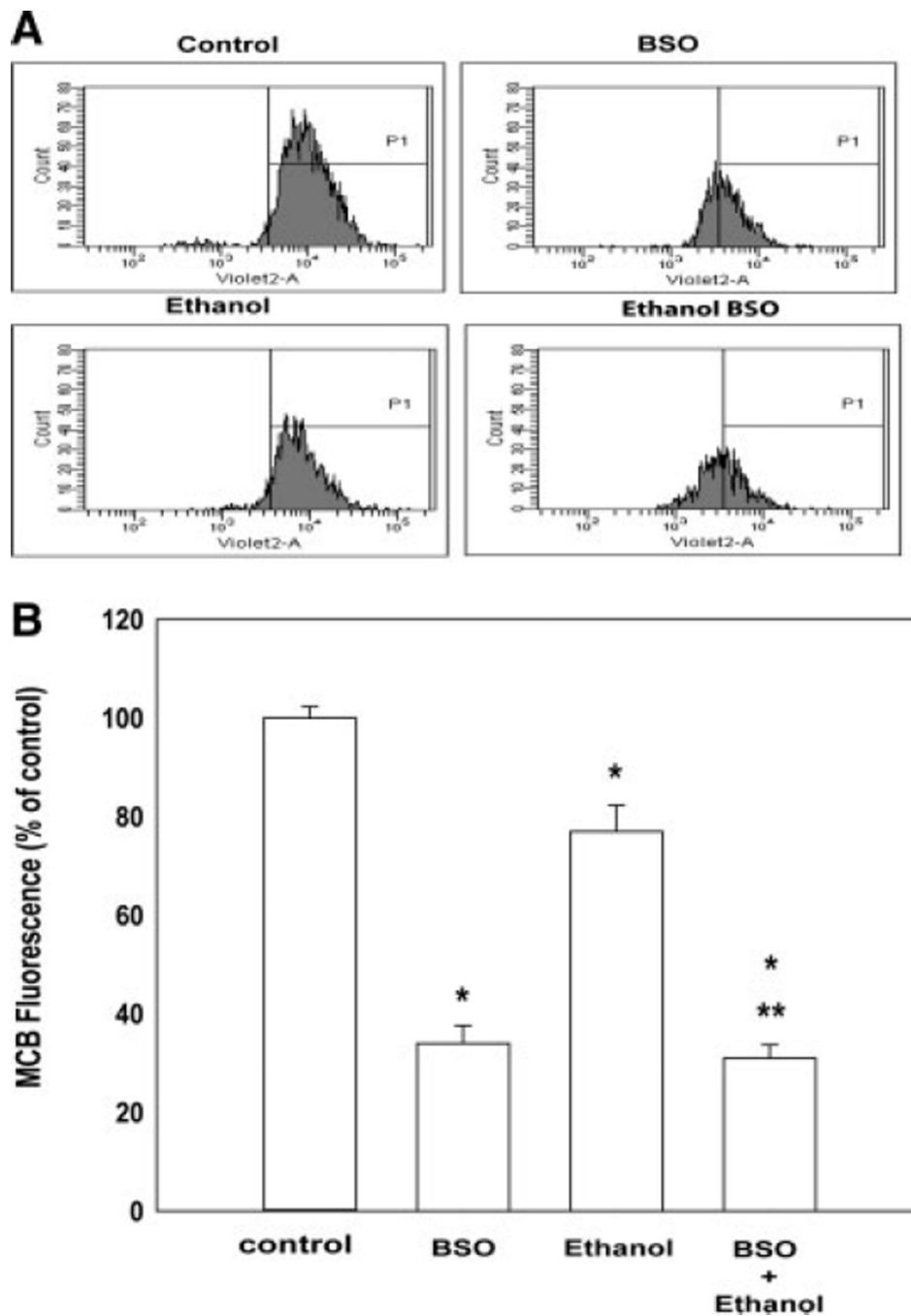
Fig. 5.
Ethanol- and BSO-related reductions of GSH content determined by flow cytometry. A: Representative flow cytometry analysis of neurons: control, GSH-depleted (200 μM BSO), ethanol-treated (4 mg/ml for 2 hr), or combined GSH-depleted and ethanol-treated. There is a broad range of intensity along the X-axis ranging from 10^2 to 10^5 units. GSH depletion, ethanol exposure, or the two in combination caused a peak shift toward the left (lower GSH content). **B**: The bar graph depicts decreases in mean intensities (GSH content) of peak P1 (% gated peak) with respect to the controls. The values are an average from three

independent experiments and are represented as mean ± SEM. $^*P< 0.01$ compared with controls. $^{**}P< 0.05$ for ethanol compared with ethanol combined with BSO.
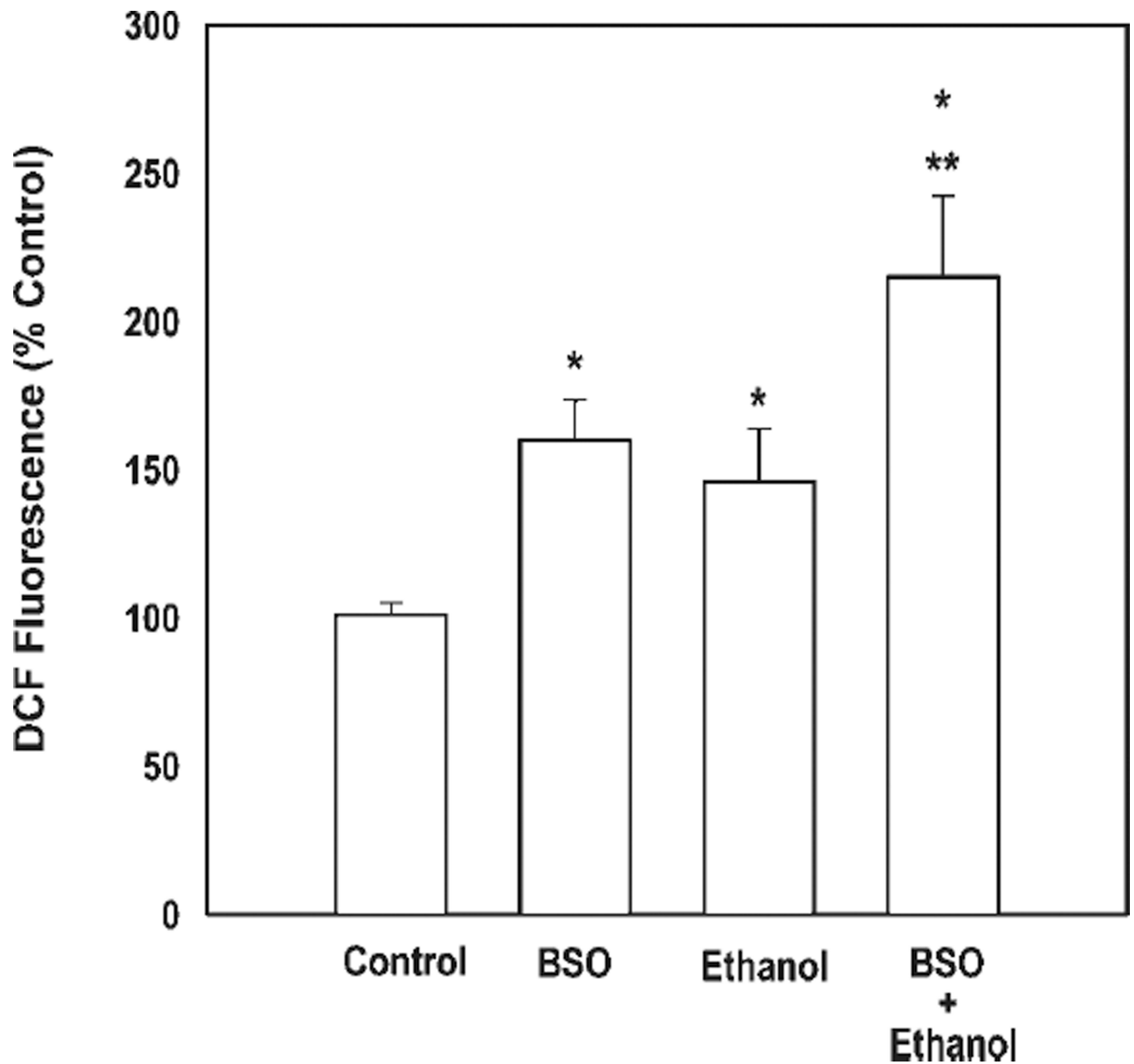
Fig. 6.
Ethanol-mediated oxidative stress is enhanced by GSH depletion. Flow cytometry experiments (10,000 events) illustrated the effects of GSH depletion, alone and in combination with ethanol, on ROS production. Neurons were depleted of GSH by overnight treatment with 200 μM BSO and/or were treated with ethanol (4 mg/ml, 2 hr). The values are an average of n = 6, represented as mean ± SEM. *Difference from controls ($P<$ 0.05). **$P<0.05$ for ethanol compared with ethanol combined with BSO.
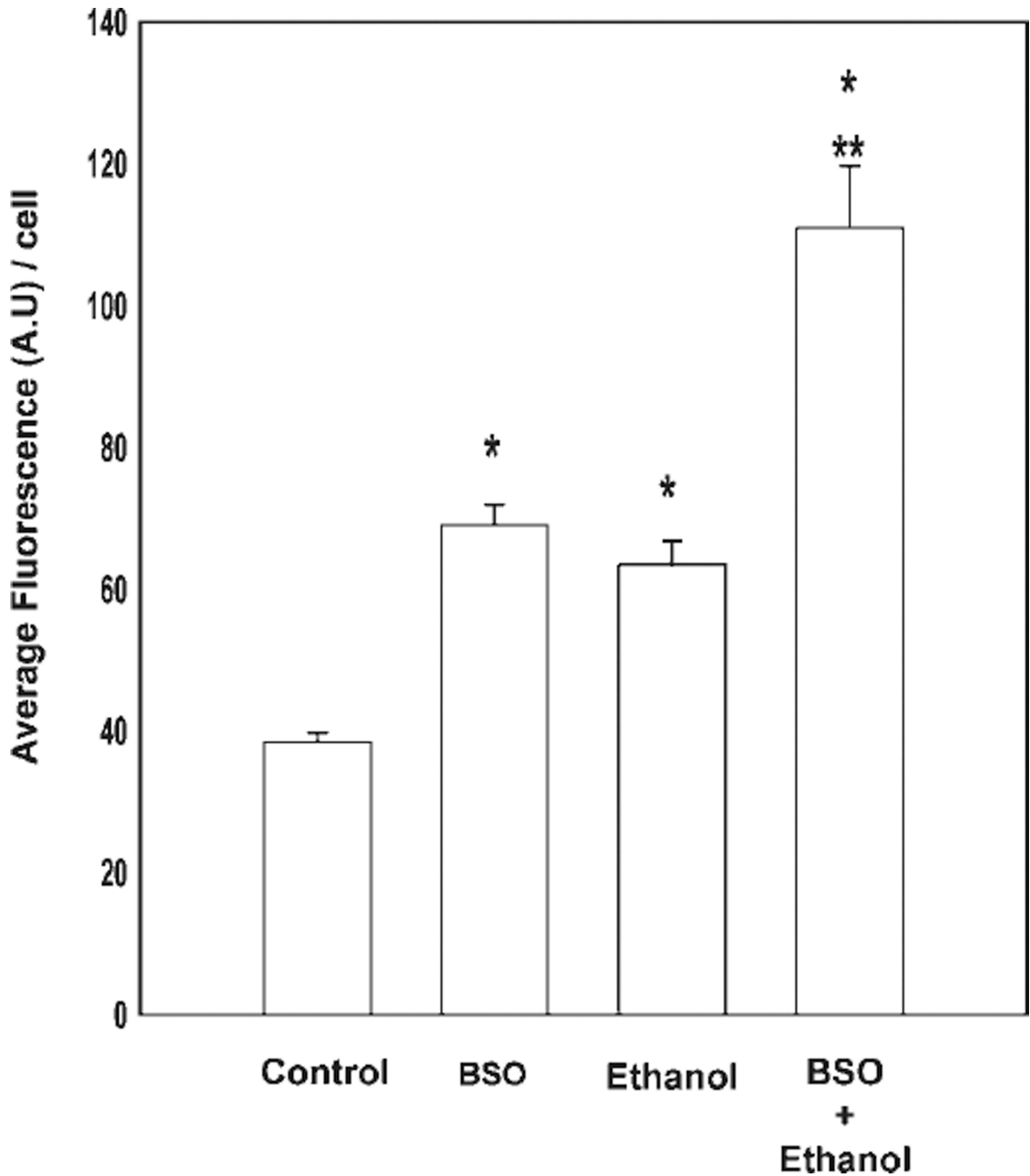
Fig. 7.
Ethanol-mediated DNA damage is enhanced by GSH depletion. Cortical neurons were grown on coverslips and assessed by TUNEL assay for DNA damage. The fluorescence intensity of each field was assessed in ImageJ and divided by the number of cells per field. Treatments consisted of control, GSH-depleted (200 μM BSO), ethanol-treated (4 mg/ml, 2 hr), and ethanol-treated cells that had been pretreated with BSO. In total, 180–225 cells were counted for each group. Values are mean fluorescence intensities/cell ± SEM from four image scans ([*]$P < 0.05$ compared with controls). [**]$P < 0.05$ for ethanol compared with ethanol combined with BSO.
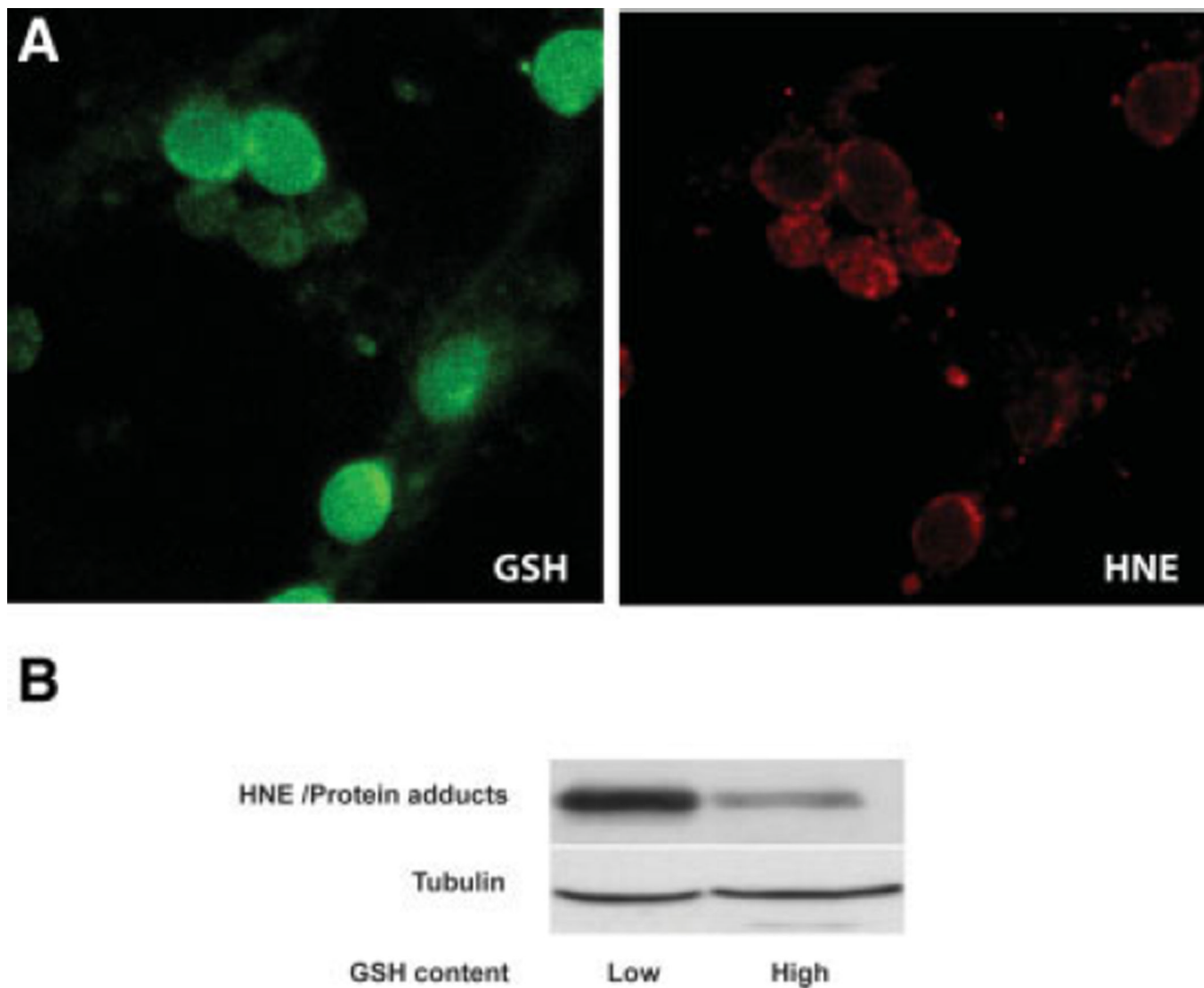
Fig. 8.
HNE-protein adduct formation is enhanced in ethanol-exposed neurons with low GSH content. A: Neurons treated with ethanol (4 mg/ml, 2 hr) and stained for GSH with MCB (green) and HNE-conjugated to Alexa 633 (red) were imaged using confocal microscopy. Neurons with high GSH content typically had less HNE adduct staining compared with those expressing low GSH-related fluorescence. **B**: Neurons treated with ethanol (4 mg/ml, 2 hr) were sorted into two subpopulations based on their GSH content: "low" for cells in the lowest 15% and "high" for cells with the 15% highest GSH content. Expression of neuronal HNE adducts (an estimate of lipid peroxidation) is amplified in the low-GSH subpopulation. Tubulin expression served as internal controls to ensure correct protein loading between lanes. This blot represents one of three similar experiments.
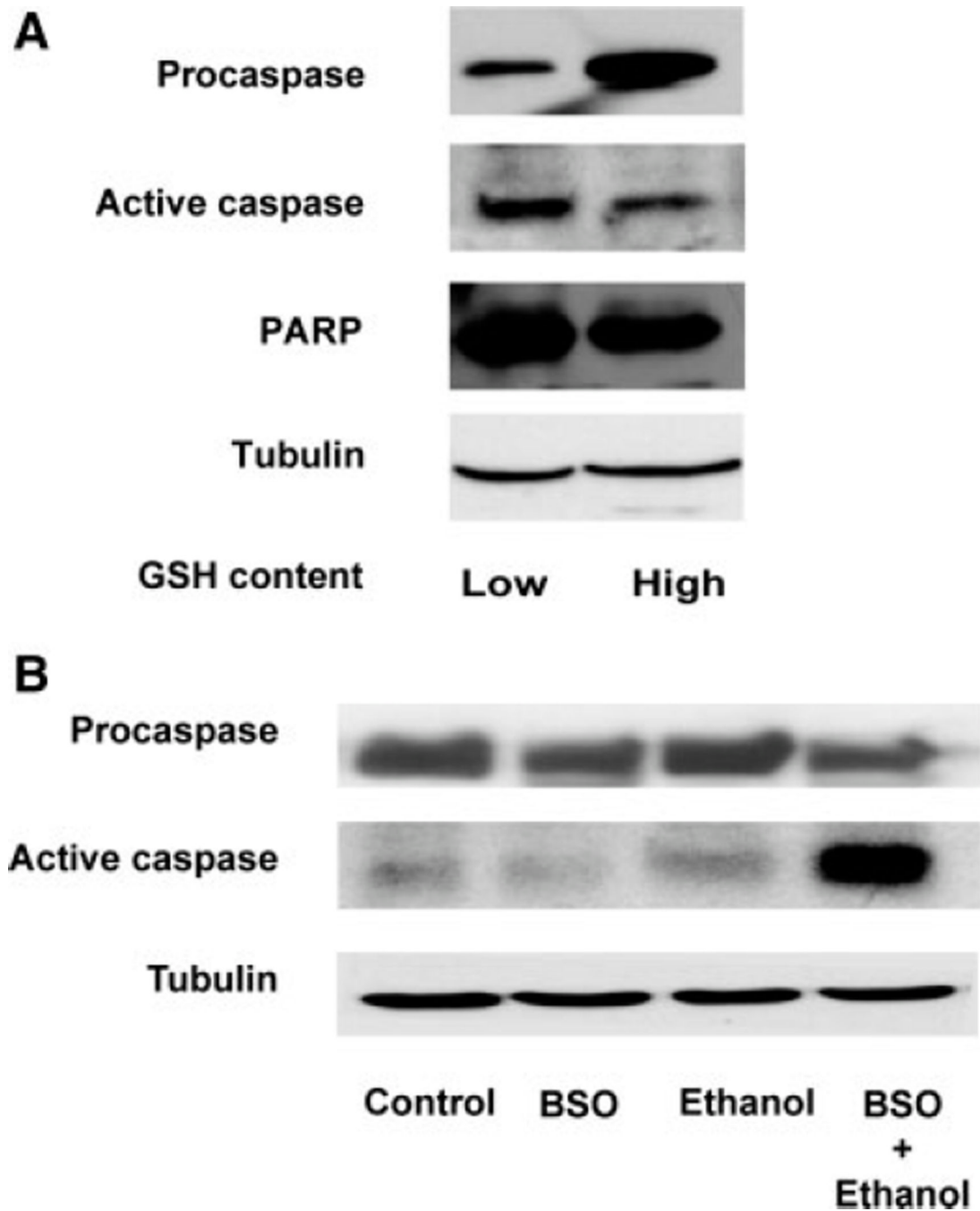
Fig. 9.
Induction of apoptosis markers is enhanced in ethanol-exposed neurons with low GSH content. **A**: Neurons were treated with ethanol (4.0 mg/ml, 2 hr), stained with MCB, and sorted by FACS. Two subpopulations based on their low and high GSH content were collected and processed for Western blotting. Compared with the high-GSH neurons, there is an increased expression of "active" caspase-3 (11-kDa fragment) and the 24-kDa PARP-1 along with a decrease in procaspase-3 in the subpopulation with low GSH content. Tubulin expression levels served as internal controls to check protein loading. This blot represents one of three similar experiments. **B**: Cultured neurons (not sorted by FACS) were treated with BSO (200 μM, 24 hr) and ethanol (4.0 mg/ml, 2 hr), then processed for Western

blotting. Expression of the 11-kDa caspase-3 fragment was increased in the ethanol-treated cells (4 mg/ml, 2 hr) and in ethanol-exposed GSH-depleted neurons. BSO, BSO treatment alone; ethanol treatment alone; BSO + Ethanol, ethanol treatment (4 mg/ml, 2 hr) and BSO (200 μM, 24 hr). Tubulin was used as the loading control. This blot represents one of three identical experiments.